

000 001 002 003 004 005 006 007 008 009 010 CAUSAL-STEER: DISENTANGLED CONTINUOUS 002 003 004 005 006 007 008 009 010 011 012 013 014 015 016 017 018 019 020 021 022 023 024 025 026 027 028 029 030 031 032 033 034 035 036 037 038 039 040 041 042 043 044 045 046 047 048 049 050 051 052 053 054 055 056 057 058 059 060 061 062 063 064 065 066 067 068 069 070 071 072 073 074 075 076 077 078 079 080 081 082 083 084 085 086 087 088 089 090 091 092 093 094 095 096 097 098 099 100 101 102 103 104 105 106 107 108 109 110 111 112 113 114 115 116 117 118 119 120 121 122 123 124 125 126 127 128 129 130 131 132 133 134 135 136 137 138 139 140 141 142 143 144 145 146 147 148 149 150 151 152 153 154 155 156 157 158 159 160 161 162 163 164 165 166 167 168 169 170 171 172 173 174 175 176 177 178 179 180 181 182 183 184 185 186 187 188 189 190 191 192 193 194 195 196 197 198 199 200 201 202 203 204 205 206 207 208 209 210 211 212 213 214 215 216 217 218 219 220 221 222 223 224 225 226 227 228 229 230 231 232 233 234 235 236 237 238 239 240 241 242 243 244 245 246 247 248 249 250 251 252 253 254 255 256 257 258 259 259 260 261 262 263 264 265 266 267 268 269 270 271 272 273 274 275 276 277 278 279 279 280 281 282 283 284 285 286 287 288 289 289 290 291 292 293 294 295 296 297 298 299 299 300 301 302 303 304 305 306 307 308 309 309 310 311 312 313 314 315 316 317 318 319 319 320 321 322 323 324 325 326 327 328 329 329 330 331 332 333 334 335 336 337 338 339 339 340 341 342 343 344 345 346 347 348 349 349 350 351 352 353 354 355 356 357 358 359 359 360 361 362 363 364 365 366 367 368 369 369 370 371 372 373 374 375 376 377 378 379 379 380 381 382 383 384 385 386 387 388 389 389 390 391 392 393 394 395 396 397 398 399 399 400 401 402 403 404 405 406 407 408 409 409 410 411 412 413 414 415 416 417 418 419 419 420 421 422 423 424 425 426 427 428 429 429 430 431 432 433 434 435 436 437 438 439 439 440 441 442 443 444 445 446 447 448 449 449 450 451 452 453 454 455 456 457 458 459 459 460 461 462 463 464 465 466 467 468 469 469 470 471 472 473 474 475 476 477 478 479 479 480 481 482 483 484 485 486 487 488 489 489 490 491 492 493 494 495 496 497 498 499 499 500 501 502 503 504 505 506 507 508 509 509 510 511 512 513 514 515 516 517 518 519 519 520 521 522 523 524 525 526 527 528 529 529 530 531 532 533 534 535 536 537 538 539 539 540 541 542 543 544 545 546 547 548 549 549 550 551 552 553 554 555 556 557 558 559 559 560 561 562 563 564 565 566 567 568 569 569 570 571 572 573 574 575 576 577 578 579 579 580 581 582 583 584 585 586 587 588 589 589 590 591 592 593 594 595 596 597 598 599 599 600 601 602 603 604 605 606 607 608 609 609 610 611 612 613 614 615 616 617 618 619 619 620 621 622 623 624 625 626 627 628 629 629 630 631 632 633 634 635 636 637 638 639 639 640 641 642 643 644 645 646 647 648 649 649 650 651 652 653 654 655 656 657 658 659 659 660 661 662 663 664 665 666 667 668 669 669 670 671 672 673 674 675 676 677 678 679 679 680 681 682 683 684 685 686 687 688 689 689 690 691 692 693 694 695 696 697 698 699 699 700 701 702 703 704 705 706 707 708 709 709 710 711 712 713 714 715 716 717 718 719 719 720 721 722 723 724 725 726 727 728 729 729 730 731 732 733 734 735 736 737 738 739 739 740 741 742 743 744 745 746 747 748 749 749 750 751 752 753 754 755 756 757 758 759 759 760 761 762 763 764 765 766 767 768 769 769 770 771 772 773 774 775 776 777 778 779 779 780 781 782 783 784 785 786 787 788 789 789 790 791 792 793 794 795 796 797 798 799 799 800 801 802 803 804 805 806 807 808 809 809 810 811 812 813 814 815 816 817 818 819 819 820 821 822 823 824 825 826 827 828 829 829 830 831 832 833 834 835 836 837 838 839 839 840 841 842 843 844 845 846 847 848 849 849 850 851 852 853 854 855 856 857 858 859 859 860 861 862 863 864 865 866 867 868 869 869 870 871 872 873 874 875 876 877 878 879 879 880 881 882 883 884 885 886 887 888 889 889 890 891 892 893 894 895 896 897 898 899 899 900 901 902 903 904 905 906 907 908 909 909 910 911 912 913 914 915 916 917 918 919 919 920 921 922 923 924 925 926 927 928 929 929 930 931 932 933 934 935 936 937 938 939 939 940 941 942 943 944 945 946 947 948 949 949 950 951 952 953 954 955 956 957 958 959 959 960 961 962 963 964 965 966 967 968 969 969 970 971 972 973 974 975 976 977 978 979 979 980 981 982 983 984 985 986 987 988 989 989 990 991 992 993 994 995 996 997 998 999 999 000 001 002 003 004 005 006 007 008 009 010 011 012 013 014 015 016 017 018 019 020 021 022 023 024 025 026 027 028 029 030 031 032 033 034 035 036 037 038 039 040 041 042 043 044 045 046 047 048 049 050 051 052 053 054 055 056 057 058 059 060 061 062 063 064 065 066 067 068 069 070 071 072 073 074 075 076 077 078 079 080 081 082 083 084 085 086 087 088 089 090 091 092 093 094 095 096 097 098 099 0100 0101 0102 0103 0104 0105 0106 0107 0108 0109 0110 0111 0112 0113 0114 0115 0116 0117 0118 0119 0120 0121 0122 0123 0124 0125 0126 0127 0128 0129 0130 0131 0132 0133 0134 0135 0136 0137 0138 0139 0140 0141 0142 0143 0144 0145 0146 0147 0148 0149 0150 0151 0152 0153 0154 0155 0156 0157 0158 0159 0160 0161 0162 0163 0164 0165 0166 0167 0168 0169 0169 0170 0171 0172 0173 0174 0175 0176 0177 0178 0179 0179 0180 0181 0182 0183 0184 0185 0186 0187 0188 0189 0189 0190 0191 0192 0193 0194 0195 0196 0197 0198 0199 0199 0200 0201 0202 0203 0204 0205 0206 0207 0208 0209 0209 0210 0211 0212 0213 0214 0215 0216 0217 0218 0219 0219 0220 0221 0222 0223 0224 0225 0226 0227 0228 0229 0229 0230 0231 0232 0233 0234 0235 0236 0237 0238 0239 0239 0240 0241 0242 0243 0244 0245 0246 0247 0248 0249 0249 0250 0251 0252 0253 0254 0255 0256 0257 0258 0259 0259 0260 0261 0262 0263 0264 0265 0266 0267 0268 0269 0269 0270 0271 0272 0273 0274 0275 0276 0277 0278 0279 0279 0280 0281 0282 0283 0284 0285 0286 0287 0288 0289 0289 0290 0291 0292 0293 0294 0295 0296 0297 0298 0299 0299 0300 0301 0302 0303 0304 0305 0306 0307 0308 0309 0309 0310 0311 0312 0313 0314 0315 0316 0317 0318 0319 0319 0320 0321 0322 0323 0324 0325 0326 0327 0328 0329 0329 0330 0331 0332 0333 0334 0335 0336 0337 0338 0339 0339 0340 0341 0342 0343 0344 0345 0346 0347 0348 0349 0349 0350 0351 0352 0353 0354 0355 0356 0357 0358 0359 0359 0360 0361 0362 0363 0364 0365 0366 0367 0368 0369 0369 0370 0371 0372 0373 0374 0375 0376 0377 0378 0379 0379 0380 0381 0382 0383 0384 0385 0386 0387 0388 0389 0389 0390 0391 0392 0393 0394 0395 0396 0397 0398 0399 0399 0400 0401 0402 0403 0404 0405 0406 0407 0408 0409 0409 0410 0411 0412 0413 0414 0415 0416 0417 0418 0419 0419 0420 0421 0422 0423 0424 0425 0426 0427 0428 0429 0429 0430 0431 0432 0433 0434 0435 0436 0437 0438 0439 0439 0440 0441 0442 0443 0444 0445 0446 0447 0448 0449 0449 0450 0451 0452 0453 0454 0455 0456 0457 0458 0459 0459 0460 0461 0462 0463 0464 0465 0466 0467 0468 0469 0469 0470 0471 0472 0473 0474 0475 0476 0477 0478 0479 0479 0480 0481 0482 0483 0484 0485 0486 0487 0488 0489 0489 0490 0491 0492 0493 0494 0495 0496 0497 0498 0499 0499 0500 0501 0502 0503 0504 0505 0506 0507 0508 0509 0509 0510 0511 0512 0513 0514 0515 0516 0517 0518 0519 0519 0520 0521 0522 0523 0524 0525 0526 0527 0528 0529 0529 0530 0531 0532 0533 0534 0535 0536 0537 0538 0539 0539 0540 0541 0542 0543 0544 0545 0546 0547 0548 0549 0549 0550 0551 0552 0553 0554 0555 0556 0557 0558 0559 0559 0560 0561 0562 0563 0564 0565 0566 0567 0568 0569 0569 0570 0571 0572 0573 0574 0575 0576 0577 0578 0579 0579 0580 0581 0582 0583 0584 0585 0586 0587 0588 0589 0589 0590 0591 0592 0593 0594 0595 0596 0597 0598 0599 0599 0600 0601 0602 0603 0604 0605 0606 0607 0608 0609 0609 0610 0611 0612 0613 0614 0615 0616 0617 0618 0619 0619 0620 0621 0622 0623 0624 0625 0626 0627 0628 0629 0629 0630 0631 0632 0633 0634 0635 0636 0637 0638 0639 0639 0640 0641 0642 0643 0644 0645 0646 0647 0648 0649 0649 0650 0651 0652 0653 0654 0655 0656 0657 0658 0659 0659 0660 0661 0662 0663 0664 0665 0666 0667 0668 0669 0669 0670 0671 0672 0673 0674 0675 0676 0677 0678 0679 0679 0680 0681 0682 0683 0684 0685 0686 0687 0688 0689 0689 0690 0691 0692 0693 0694 0695 0696 0697 0698 0699 0699 0700 0701 0702 0703 0704 0705 0706 0707 0708 0709 0709 0710 0711 0712 0713 0714 0715 0716 0717 0718 0719 0719 0720 0721 0722 0723 0724 0725 0726 0727 0728 0729 0729 0730 0731 0732 0733 0734 0735 0736 0737 0738 0739 0739 0740 0741 0742 0743 0744 0745 0746 0747 0748 0749 0749 0750 0751 0752 0753 0754 0755 0756 0757 0758 0759 0759 0760 0761 0762 0763 0764 0765 0766 0767 0768 0769 0769 0770 0771 0772 0773 0774 0775 0776 0777 0778 0779 0779 0780 0781 0782 0783 0784 0785 0786 0787 0788 0789 0789 0790 0791 0792 0793 0794 0795 0796 0797 0798 0799 0799 0800 0801 0802 0803 0804 0805 0806 0807 0808 0809 0809 0810 0811 0812 0813 0814 0815 0816 0817 0818 0819 0819 0820 0821 0822 0823 0824 0825 0826 0827 0828 0829 0829 0830 0831 0832 0833 0834 0835 0836 0837 0838 0839 0839 0840 0841 0842 0843 0844 0845 0846 0847 0848 0849 0849 0850 0851 0852 0853 0854 0855 0856 0857 0858 0859 0859 0860 0861 0862 0863 0864 0865 0866 0867 0868 0869 0869 0870 0871 0872 0873 0874 0875 0876 0877 0878 0879 0879 0880 0881 0882 0883 0884 0885 0886 0887 0888 0889 0889 0890 0891 0892 0893 0894 0895 0896 0897 0898 0899 0899 0900 0901 0902 0903 0904 0905 0906 0907 0908 0909 0909 0910 0911 0912 0913 0914 0915 0916 0917 0918 0919 0919 0920 0921

054 anchor training and tends to capture corpus-specific artifacts rather than genuine stylistic differences.
 055 Consequently, the model merges dataset features instead of learning a transferable representation of
 056 style, resulting in outputs that are unstable and difficult to control.
 057

058 To address these gaps, the emerging paradigm of **activation steering** has attracted increasing at-
 059 tention (Turner et al., 2023a; Zhang et al., 2025). By directly manipulating a model’s internal
 060 representations in latent space, activation steering offers a principled mechanism for **continuous,**
 061 **fine-grained control** over stylistic attributes. However, the practical effectiveness of this approach
 062 hinges on obtaining high-quality steering directions. Existing methods typically rely on *parallel*
 063 *corpora*(Han et al., 2024), pairs of texts aligned in content but differing in style, which are expen-
 064 sive to construct and rarely available for complex dimensions such as conceptual complexity. This
 065 dependence introduces two critical challenges. First, the **content pollution problem**: imperfect
 066 content alignment causes extracted difference vectors to encode both stylistic and semantic varia-
 067 tion, reducing generalizability. Second, the **robustness problem**: even when initial style signals are
 068 isolated, steering directions remain vulnerable to noise and outliers, limiting stability across topics.
 069

070 In this work, we present a novel framework, Causal-Steer, for robust, corpus-free activation steering
 071 that enables precise and linear style control. Our key insight is to reframe Low-Rank Adaptation (Hu
 072 et al., 2022) (LoRA) as a **causal intervention tool**. By contrasting activations from identical inputs
 073 with and without a LoRA perturbation, we isolate the net stylistic effect while circumventing the
 074 need for parallel data. To further enhance reliability, we design an aggregation pipeline that applies
 075 PCA for denoising and employs robust centrality estimation to derive stable steering vectors resilient
 076 to outliers. Using conceptual complexity as a case study, we demonstrate that our method supports
 077 continuous bidirectional control and generalizes across tasks and languages.
 078

079 Our main contributions are as follows:
 080

1. **Linear, Corpus-Free Bidirectional Control.** We extract a style vector from a single, non-parallel dataset (even a single-style dataset) and leverage it to realize fine-grained, linear, and bidirectional control, removing the need for costly parallel corpora.
2. **Robust and Disentangled Representation.** Through PCA-based denoising and robust centrality aggregation, our method suppresses content-related noise and resists outliers, producing a disentangled style vector that remains stable and transferable across diverse settings.
3. **Versatile, State-of-the-Art Performance.** Causal-Steer outperforms prior methods on multiple tasks such as text detoxification and formality control, and consistently generalizes to different domains and languages without additional tuning.

087 2 RELATED WORK

088 Approaches to style control in LLMs can be broadly categorized into modifications of model param-
 089 eters (Mañas et al., 2025; Feng et al., 2025) and inference-time activations (Feng et al., 2024; Klein
 090 & Nabi, 2024). In the parameter space, Ilharco et al. (2022) introduced “task arithmetic”, where vec-
 091 tors derived from fine-tuning are used to edit model capabilities (Akiba et al., 2025). More directly
 092 related to style, Dekoninck et al. (2023) demonstrated that interpolating between multiple LoRA
 093 adapters, each fine-tuned on different attributes, can effectively control generation style. An alter-
 094 native, more lightweight paradigm is activation engineering. Pioneering this, Turner et al. (2023a)
 095 developed Activation Addition (ActAdd), computing a steering vector from the activation difference
 096 of a single pair of contrasting prompts. This concept was refined by Rimsky et al. (2024) with Con-
 097 trastive Activation Addition (CAA), which averages these differences over a large dataset of pairs
 098 for greater stability. In a similar vein, Zhang et al. (2025) proposed Generation with Concept Acti-
 099 vation Vectors (GCAV), deriving a controlling vector by training a linear classifier on activations. For
 100 more targeted edits, Li et al. (2023) developed Inference-Time Intervention (ITI) to shift activations
 101 in specific truth-related attention heads. Finally, Zou et al. (2023) unified these activation-based
 102 approaches under the conceptual framework of Representation Engineering.
 103

104 3 METHODOLOGY

105 To separate the extracted style vector $\mathbf{v}_{\text{style}}$ from content and mitigate interference from style noise,
 106 we aim to achieve fine-grained linear control over text style. Causal-Steer as show in Figure 2,
 107

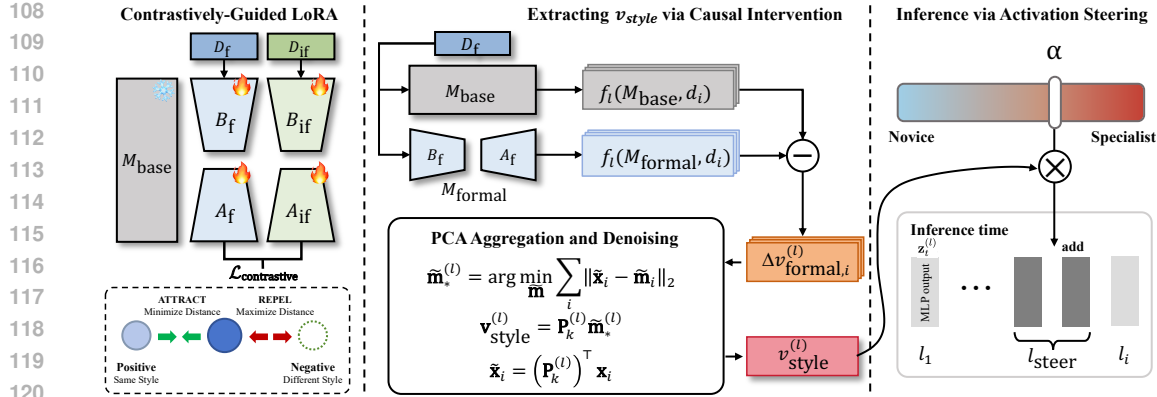


Figure 2: **Framework for extracting and controlling style.** The process is (1) training style-specific LoRAs with a contrastive loss, (2) extracting perturbations caused by the LoRAs and aggregating them into v_{style} , and (3) using this vector for continuous style control at inference. Here, D_f and D_{if} denote the formal and informal datasets; B_f , A_f , B_{if} , and A_{if} are the corresponding LoRA modules; M_{base} is the base model; $f_l(\cdot)$ is the activation extraction function; l_{steer} is the steering layer; $\Delta v^{(l)}$ is the per-example activation perturbation; and v_{style} is the aggregated style vector.

consists of three main stages: 1) We use a contrastively-guided LoRA to introduce a precise, low-rank perturbation to the base model’s weights and extract style-specific activation differences from the perturbation. 2) We introduce a robust aggregation technique that combines PCA with a robust centrality estimation to denoise the extracted vectors and identify the core style direction. 3) At inference time, we use the normalized style vector for multi-layer activation steering, enabling continuous and fine-grained style control.

3.1 PRELIMINARIES

Base and Perturbed Models. M_{base} is a frozen pretrained language model. M_{formal} and $M_{informal}$ are models obtained by applying LoRA-based perturbations to M_{base} , trained on style-specific datasets D_{formal} and $D_{informal}$ respectively, using a contrastive loss. Crucially, these datasets need not be parallel, the only requirement is that they exhibit contrasting styles.

MLP-Layer Activation Extractor. For a Transformer layer l , a model M , and a text d , we define $f_l(M, d)$ as the mean of the MLP output vectors for all generated tokens, excluding prompt tokens:

$$f_l(M, d) = \frac{1}{T_r} \sum_{t=1}^{T_r} \mathbf{z}_t^{(l)}, \quad (1)$$

where $\mathbf{z}_t^{(l)}$ is the post-MLP hidden state for the t -th token, and T_r is the number of generated tokens. This design ensures that the extracted style vector reflects holistic stylistic features throughout the model’s output, rather than structural artifacts from the prompt or the partial semantic biases of individual tokens.

3.2 EXTRACTING STYLE VECTORS VIA CAUSAL INTERVENTION

LoRA fundamentally applies a precise, low-rank update ΔW to the base model’s weights W_0 , resulting in fine-tuned weights $W_{style} = W_0 + \Delta W$. We treat this fine-tuning process as a precise **causal intervention** on the model. Its goal is to elicit specific stylized behaviors while avoiding significant shifts in the core semantic space learned during pretraining. To ensure this perturbation ΔW effectively separates style from content, we guide its training with a **contrastive learning objective**. This objective directs the weight update towards a subspace that maximizes style separability. Specifically, the objective function to guide the M_{formal} perturbation is:

$$\mathcal{L}_{\text{contrastive}} = -\mathbb{E} \left[\log \frac{\exp(\text{sim}(\mathbf{h}_{d_a}, \mathbf{h}_{d_p})/\tau)}{\exp(\text{sim}(\mathbf{h}_{d_a}, \mathbf{h}_{d_p})/\tau) + \sum_{d_n} \exp(\text{sim}(\mathbf{h}_{d_a}, \mathbf{h}_{d_n})/\tau)} \right], \quad (2)$$

162 where the anchor \mathbf{h}_{d_a} and positive example \mathbf{h}_{d_p} are from D_{formal} , and negative examples \mathbf{h}_{d_n} are
 163 from D_{informal} . This discriminative guidance compels the LoRA update ΔW to focus on generaliz-
 164 able features that can distinguish the two styles across different content. Consequently, the model
 165 must suppress content-related activations, thereby learning a pure and generalizable style represen-
 166 tation. We employ a differential method to extract the pure effect of this stylistic perturbation. For a
 167 formal sample d_i and layer l , the stylistic perturbation vector is defined as:

$$\Delta \mathbf{v}_{\text{formal},i}^{(l)} = f_l(M_{\text{formal}}, d_i) - f_l(M_{\text{base}}, d_i). \quad (3)$$

170 The informal difference vector $\Delta \mathbf{v}_{\text{informal},j}^{(l)}$ is calculated analogously.
 171

172 This differential measurement approach is fundamentally different from naive observational meth-
 173 ods. A baseline approach would be to directly obtain the style vector from the difference in activa-
 174 tions on the datasets D_{formal} and D_{informal} within the base model M_{base} . However, this method
 175 assumes that content-related information can be eliminated via vector subtraction, thereby isolating
 176 the pure style signal. This assumption holds only under the condition of extremely high content
 177 consistency between texts, which in turn necessitates a meticulously crafted parallel corpus. Causal-
 178 Steer, in contrast, captures the LoRA-induced perturbation on the very same input d_i , elegantly
 179 circumventing this reliance on parallel corpora.

180 Causal-Steer’s ability to isolate the stylistic effect hinges on the approximately linear relationship
 181 between the weight perturbation ΔW and the change in activations. We formalize this relationship
 182 by considering the activation of layer l as a function of weights W and data d , denoted as $\mathbf{h}^{(l)}(W, d)$.
 183 A first-order Taylor expansion around the base weights W_0 yields:

$$\Delta \mathbf{h}^{(l)}(d) = \mathbf{h}^{(l)}(W_0 + \Delta W, d) - \mathbf{h}^{(l)}(W_0, d) \approx J_{\mathbf{h}, W}(W_0, d) \cdot \Delta W, \quad (4)$$

184 where $J_{\mathbf{h}, W}(W_0, d) = \frac{\partial \mathbf{h}^{(l)}(W, d)}{\partial W} \Big|_{W=W_0}$ is the Jacobian matrix mapping perturbations in the weight
 185 space to changes in the activation space.

186 This linear approximation indicates that the $\Delta \mathbf{h}^{(l)}$ we extract can be interpreted as the image of
 187 the LoRA-induced weight perturbation ΔW under this Jacobian mapping. In other words, $\Delta \mathbf{h}^{(l)}$
 188 represents how the stylistic intervention in the weight space manifests within the model’s hidden
 189 representation space, thus providing a direct and disentangled handle for controlling style.

193 3.3 ROBUST AGGREGATION AND DENOISING

194 Our objective is to aggregate the collected sample-level difference vectors for each layer into a sin-
 195 gle, robust style vector $\mathbf{v}_{\text{style}}^{(l)}$. A simple baseline, the arithmetic mean, is suboptimal as it conflates
 196 the primary style signal with sample-specific content variations. This indiscriminate averaging in-
 197 troduces noise and fails to isolate the core style direction. To address this, we propose a two-stage
 198 strategy that first denoises the vectors to isolate the style subspace and then performs a robust aggre-
 199 gation within that subspace.

200 **Vector Set Construction and Modeling.** We first construct a unified set of style difference vectors
 201 by aligning their directions. Specifically, we negate the vectors derived from the informal style to
 202 align them with the formal style direction:

$$X^{(l)} = \{\Delta \mathbf{v}_{\text{formal}}^{(l)}\} \cup \{-\Delta \mathbf{v}_{\text{informal}}^{(l)}\}. \quad (5)$$

203 We model each vector $\mathbf{x}_i \in X^{(l)}$ as a composition of a shared, low-dimensional style signal $\mathbf{v}_{\text{style}}^{(l)}$
 204 and high-dimensional, sample-specific content noise $\epsilon_{\text{content},i}$:

$$\mathbf{x}_i = \mathbf{v}_{\text{style}}^{(l)} + \epsilon_{\text{content},i}. \quad (6)$$

205 This model posits that the consistent style direction is the primary signal shared across all samples,
 206 whereas content-related features manifest as diverse noise.

207 **Denoising via PCA.** Based on our model, we hypothesize that the shared style signal $\mathbf{v}_{\text{style}}^{(l)}$ consti-
 208 tutes the principal components with the highest variance in the set $X^{(l)}$. Conversely, the content
 209 noise $\epsilon_{\text{content},i}$ is distributed across the remaining components of lower variance. Consequently, we

216
217 Table 1: Evaluation results on conceptual complexity. Methods with the mean suffix utilize mean
218 token feature extraction for control. Among these, RepE_{mean} failed and is excluded from the ranking,
219 **CS** denotes our **Causal-Steer** method, and **CS_{single}** denotes the variant trained only on the single
220 sided (simple) dataset. For all successful methods, the best results are in **bold** and the second best
221 are underlined. Arrows ($\uparrow\downarrow$) indicate the desired direction for each metric. **All ChatGPT-4.1-based**
222 **metrics are scored on a 1–10 scale.**

Method	Model	Complex							Simple						
		Rel. \uparrow	Flu. \uparrow	Acc. \uparrow	Diff. \uparrow	F-G. \uparrow	<u>SMOG.</u> \uparrow	<u>C-L.</u> \uparrow	Rel. \uparrow	Flu. \uparrow	Acc. \uparrow	Diff. \downarrow	F-G. \downarrow	<u>SMOG.</u> \downarrow	<u>C-L.</u> \downarrow
CAA	Qwen	9.56	8.71	8.19	5.37	16.28	15.57	15.64	9.57	8.51	7.58	4.18	13.64	11.19	15.71
ITI	2.5-7B	9.75	9.08	8.48	5.16	16.64	15.05	15.45	9.67	8.73	7.83	4.17	13.78	17.48	17.14
RepE	-Instruct	9.60	8.76	8.24	5.35	16.28	14.83	14.84	9.71	8.73	8.17	4.37	14.52	17.23	17.93
CAA _{mean}		9.53	8.26	7.91	8.00	19.98	19.24	<u>29.08</u>	9.01	8.36	6.59	2.85	11.97	12.07	10.81
RepE _{mean}		9.81	9.12	8.41	4.99	16.57	15.67	17.59	9.83	9.13	8.68	4.82	14.98	15.00	14.41
ITI _{mean}	Qwen	9.78	8.41	8.30	6.97	18.25	18.03	22.06	8.94	7.87	6.71	3.12	11.92	12.52	10.80
CLMI	2.5-7B	8.92	7.97	7.60	8.36	20.67	22.49	26.91	9.50	9.06	7.64	3.47	11.38	11.37	10.02
ReFT	-Instruct	8.96	8.31	7.78	4.11	12.38	14.20	13.46	8.26	7.91	6.87	3.05	12.24	11.23	9.89
CS		9.75	8.35	8.59	8.42	<u>22.78</u>	<u>21.97</u>	31.55	<u>9.29</u>	<u>8.41</u>	<u>6.85</u>	2.77	10.71	9.05	7.46
CS _{single}		9.67	8.30	<u>8.56</u>	8.40	23.95	21.14	27.28	9.16	8.34	6.76	<u>2.80</u>	<u>10.33</u>	<u>10.89</u>	<u>9.74</u>
CAA _{mean}		8.35	6.91	5.53	6.62	20.04	19.68	21.60	6.64	4.89	4.01	<u>1.97</u>	12.69	<u>10.80</u>	9.98
RepE _{mean}		9.24	8.30	6.92	4.33	14.48	15.89	16.25	9.35	8.37	6.66	4.25	13.60	14.45	15.03
ITI _{mean}	LLaMa	9.06	7.54	6.33	5.98	18.65	18.90	19.88	6.56	4.98	3.74	2.08	8.27	10.04	9.42
CLMI	3.1-8B	9.17	8.28	8.15	6.63	19.00	20.05	<u>26.86</u>	9.41	9.29	7.26	2.96	9.54	10.69	8.67
ReFT	-Instruct	7.29	7.25	6.30	3.12	3.12	11.19	8.15	<u>8.05</u>	<u>8.80</u>	<u>5.71</u>	2.31	<u>7.31</u>	<u>9.76</u>	<u>7.27</u>
CS		9.53	8.34	7.44	7.22	<u>20.54</u>	22.54	29.52	6.88	6.58	4.06	1.92	6.16	8.02	6.97
CS _{single}		9.59	<u>8.31</u>	<u>7.94</u>	7.81	<u>21.63</u>	<u>20.17</u>	24.64	8.04	7.61	5.18	2.16	9.04	10.22	8.79

236
237 employ PCA to separate the style signal from the content noise. We project each vector \mathbf{x}_i in $X^{(l)}$
238 onto the subspace spanned by the top k principal components:

$$\tilde{\mathbf{x}}_i = (\mathbf{P}_k^{(l)})^\top \mathbf{x}_i, \quad (7)$$

241 where the columns of $\mathbf{P}_k^{(l)}$ are the top k eigenvectors of the sample covariance matrix. This pro-
242 jection acts as a filter, preserving the low-dimensional style information while discarding high-
243 dimensional content variations. Empirically, we find that a small value such as $k = 8$ is sufficient to
244 capture the core style variance, supporting our hypothesis that style is a low-dimensional attribute.

245 **Robust Aggregation with Geometric Median.** While PCA removes structural noise, outliers from
246 atypical samples may persist within the projected style subspace. To mitigate their influence, we
247 perform a robust aggregation using the Geometric Median $\tilde{\mathbf{m}}_*^{(l)}$, which is defined as:

$$\tilde{\mathbf{m}}_*^{(l)} = \arg \min_{\tilde{\mathbf{m}}} \sum_i \|\tilde{\mathbf{x}}_i - \tilde{\mathbf{m}}\|_2. \quad (8)$$

251 Unlike the arithmetic mean, the geometric median provides a robust measure of centrality that is less
252 sensitive to extreme values. Finally, we project the aggregated vector back to the original activation
253 space to obtain the definitive style vector:

$$\mathbf{v}_{\text{style}}^{(l)} = \mathbf{P}_k^{(l)} \tilde{\mathbf{m}}_*^{(l)}. \quad (9)$$

254 This two-stage procedure yields a robust style vector that generalizes across diverse inputs, enabling
255 reliable and controllable style steering at inference time.

256 3.4 STYLE CONTROL AT INFERENCE VIA ACTIVATION STEERING

259 A key advantage of Causal-Steer is its ability to enable bidirectional control from a single style vec-
260 tor. This vector can be extracted from a non-parallel corpus representing only the target property
261 (e.g., complex concepts), yet it can steer generation towards or away from that property. We achieve
262 this control at inference time via activation steering, a method that directly modifies a model’s inter-
263 nal activations without altering its weights.

264 Specifically, for a selected set of layers $\mathcal{L}_{\text{steer}}$ (see Section 4.3 for selection details), we intervene in
265 the output of the MLP submodule during the generation of each token t . We add the pre-computed,
266 normalized style vector $\mathbf{v}_{\text{style}}^{(l)}$ to the original activation $\mathbf{z}_t^{(l)}$, scaled by an intensity coefficient α :

$$\mathbf{z}'^{(l)}_t = \mathbf{z}^{(l)}_t + \alpha \cdot \frac{\mathbf{v}_{\text{style}}^{(l)}}{\|\mathbf{v}_{\text{style}}^{(l)}\|_2}. \quad (10)$$

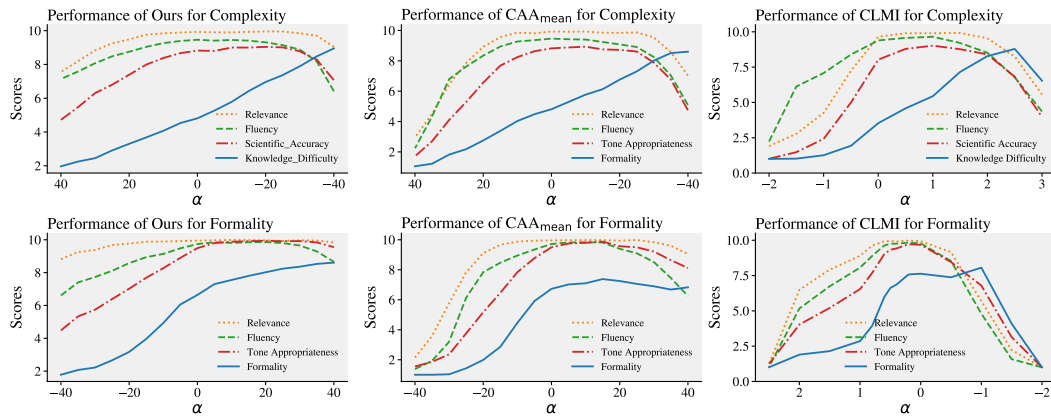


Figure 3: A comparison of the control effectiveness of Causal-Steer against two baselines on Complexity and Formality tasks. The results demonstrate that by adjusting the coefficient α , Causal-Steer effectively steers the target style while maintaining high scores for Relevance and Fluency.

Here, $\mathbf{v}_{\text{style}}^{(l)}$ is the robust style vector derived previously. We normalize it to ensure that the intervention strength is determined solely by the tunable scalar α .

The coefficient α provides continuous and fine-grained control over the output’s complexity level. A positive α guides the model towards the target property (e.g., complex), whereas a negative α steers the activations in the opposite direction (e.g., simple). When $\alpha = 0$, the original model behavior is recovered as the activations remain unchanged. This method transforms complexity control into a single, interpretable parameter. Since style vectors are pre-computed, the intervention is a simple vector addition with negligible computational overhead. This makes the method highly efficient and flexible, allowing for smooth interpolation of concept complexity without any model retraining.

4 EXPERIMENTS

Datasets. We evaluate Causal-Steer on three stylistic control tasks: conceptual complexity, toxicity detoxification, and formality control. For our primary task of conceptual complexity, we extract style vectors from the **Scale** dataset (Wang et al., 2025) and evaluate on the **ELI5** dataset (Fan et al., 2019). To assess generalization, we test toxicity control using vectors from **APPDIA** (Atwell et al., 2022) on the **RealToxicityPrompts** corpus (Gehman et al., 2020), and formality control using data from Zhang et al. (2020) evaluated on **ELI5**. Further details on data preprocessing and statistics are provided in the Appendix D.

Baselines. We benchmark Causal-Steer against a comprehensive suite of baselines including Representation Engineering (RepE) (Zou et al., 2023), Contrastive Activation Addition (CAA) (Turner et al., 2023a), Inference-Time Intervention (ITI) (Li et al., 2023), Continuous Language Model Interpolation (CLMI) (Kangaslahti & Alvarez-Melis, 2025), ReFT (Wu et al.), POSPROMPT, Arithmetic (Dekoninck et al., 2023), ActAdd (Turner et al., 2023b), and GCAV-Output (Zhang et al., 2025). Further details on each baseline are provided in the Appendix C.

Evaluation Metrics. For conceptual complexity control, we assess Relevance, Fluency, Scientific Accuracy, and Knowledge Difficulty using ChatGPT-4.1 (OpenAI, 2025), supplemented by the automated Flesch Grade Level (Flesch, 2007), SMOG (Mc Laughlin, 1969), Coleman-Liau (Coleman & Liau, 1975), and human evaluation in the Appendix E. For formality control, we evaluate Tone Appropriateness, Relevance, Fluency, and Formality using GPT-4.1. We also use the popular s-

324 nlp/roberta-base-formality-ranker model¹ from Hugging Face as the text formality style prediction
 325 model. This is a binary classification model, and we use the probability value as the text formal style
 326 strength. Finally, detoxification performance is measured by the maximum toxicity score from the
 327 Perspective API². Full evaluation prompts are detailed in the Appendix G.

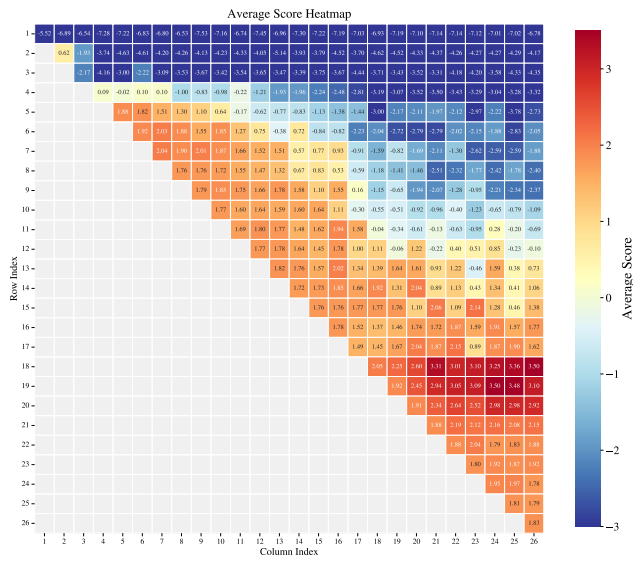
328 For the ChatGPT-4.1 metrics, we conducted three measurements and reported their average. Because
 329 the ChatGPT-4.1 scores were highly consistent, the standard deviations across the three runs were
 330 very small. Due to space constraints, we report only the average values and omit the standard
 331 deviations. All scores range from 1 to 10.

334 4.1 MAIN RESULTS ON CONCEPTUAL COMPLEXITY CONTROL

337 Table 1 presents the quantitative
 338 results for controlling conceptual com-
 339 plexity. Causal-Steer significantly
 340 outperforms most baselines across
 341 both the Qwen2.5-7B-Instruct(Qwen
 342 et al., 2024) and LLaMa3.1-8B-
 343 Instruct(Grattafiori et al., 2024). The
 344 framework demonstrates strong style
 345 control while maintaining high gen-
 346 eration quality. When steering to-
 347 wards “Complex”, Causal-Steer ex-
 348 hibits superior control. On Qwen2.5-
 349 7B, for instance, it achieves the high-
 350 est difficulty score (8.42) and Flesch
 351 grade (22.78), producing conceptually
 352 advanced content without sac-
 353 rificing relevance or fluency. Con-
 354 versely, for the “Simple” condition,
 355 Causal-Steer consistently records the
 356 lowest difficulty and Flesch grade
 357 scores. These results confirm our
 358 vector’s capacity for precise bidirec-
 359 tional steering.

360 The analysis of the baselines reveals
 361 the importance of our activation strat-
 362 egy. Methods like the original CAA, ITI, and RepE rely on activations from the final token. This
 363 approach necessitates high-quality parallel corpora to be effective. As shown in the table, adapting
 364 CAA to use mean activations (CAA_{mean}) substantially enhances its control capabilities. In contrast,
 365 RepE_{mean} still fails. We attribute this failure to its use of PCA for analyzing activations, a technique
 366 that requires a much larger dataset to identify a meaningful style direction. This hypothesis is sup-
 367 ported by our generalization experiments, where its performance improves on the larger Formality
 368 dataset (16,000 examples) (Zhang et al., 2020).

369 Although CLMI achieves commendable results in style control, its primary limitation is a failure to
 370 disentangle style from content during fine-tuning. Consequently, the model learns to associate the
 371 target style with specific content from its training data, leading to the generation of content artifacts.
 372 CLMI’s outputs are consistently shorter (approx. 100 tokens) than those of other methods (approx.
 373 500 tokens), mirroring its training data in both length and structure. This highlights that Causal-
 374 Steer succeeds by isolating a pure style vector. This isolation enables robust, generalizable control,
 375 which is unachievable by other methods that suffer from severe content-style entanglement.



376 **Figure 4: Heatmap of average style control scores across**
 377 **layer blocks.** The y-axis and x-axis represent the start and
 378 end indices for the intervention block, respectively. Scores
 379 are averaged over multiple runs.

380 ¹<https://huggingface.co/s-nlp/roberta-base-formality-ranker>

381 ²<https://perspectiveapi.com>

378
379

4.2 SINGLE-SOURCE BIDIRECTIONAL CONTROL

380
381
382
383
384
385
386
387
388

Beyond the standard setting with two style-specific LoRA adapters, Causal-Steer also supports bidirectional control when both the adapter and the steering vector are learned from a single-sided corpus. To verify this, we construct a variant, denoted $\text{CS}_{\text{single}}$, that uses only the *Simple* subset of the Scale dataset. In this variant, we remove the contrastive loss used in Section 3 and fine-tune a *single* LoRA on Simple answers with the standard supervised objective. We then apply the same causal-intervention procedure to extract one style vector. At inference time, we use a positive steering coefficient $\alpha > 0$ for the learned style and a negative coefficient $\alpha < 0$ to steer in the opposite (more complex) direction. As shown in Table 1, $\text{CS}_{\text{single}}$ achieves remarkable performance, effectively demonstrating robust bidirectional control even when trained on single-sided data.

389
390
391
392
393
394
395
396
397

We further compare this single-source setting against ReFT. While ReFT performs well when steering in the learned direction (positive scaling), it fails significantly when we attempt bidirectional control. Specifically, applying a negative coefficient for ReFT does not yield the opposite style; instead, it leads to severe generation artifacts, such as repetition and hallucinations, without successfully shifting the style. We hypothesize that this failure stems from the nature of the learned representation: ReFT likely learns a vector representing the *residual* between the base model and the dataset outputs, rather than an intrinsic *style vector*. Consequently, simply reversing this residual is semantically meaningless, causing model collapse. In contrast, our method explicitly learns the *style vector itself*, thereby enabling stable and valid bidirectional control.

398
399

4.3 ANALYSIS OF THE CONTROL MECHANISM

400
401

To better understand the properties of Causal-Steer, we conduct a deeper analysis of its control linearity and layer-wise sensitivity.

402

Linear and Stable Stylistic Control.

A core objective of Causal-Steer is to enable continuous and predictable control over style. Figure 3 evaluates this by plotting performance metrics against the steering coefficient α . The results for Causal-Steer demonstrate a strong, approximately linear relationship between α and the target style metrics, Formality and Knowledge Difficulty. As α increases, the intended stylistic intensity grows predictably. Critically, this control is achieved with minimal impact on generation quality. Key metrics such as Relevance and Fluency remain high across a wide operational range of α values, showing degradation only at extreme settings. This stability highlights the effectiveness of our robust aggregation pipeline.

419

The CLMI reveals a more fundamental limitation. Its control is effectively confined to the spectrum between its two training endpoints, corresponding to a safe operational range for α between 0 and 1. Because this method functions by interpolating between the weights of two fine-tuned models, it cannot extrapolate beyond the styles observed during training. Attempting to push the model outside this bounded range, for instance, by setting α to values like -1 or 2, results in a catastrophic collapse in generation quality, causing all performance metrics to plummet. This means the method cannot generate content that is, for example, more formal than the examples in its formal dataset without sacrificing coherence. This fundamentally restricts its utility to a narrow style range and prevents true creative or intensified style generation. The comparison confirms the superiority of Causal-Steer in creating a genuinely continuous, wide-ranging, and robust control mechanism.

429

Identifying Optimal Layers for Intervention. We investigate which layers are most influential for style control to inform an optimal intervention strategy. Figure 6 visualizes the average style score achieved by applying our steering vector across different continuous blocks of layers, defined

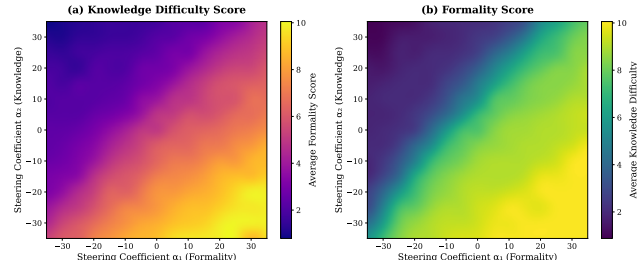


Figure 5: **Two-Dimensional Stylistic Control.** Model output scores for (a) Knowledge Difficulty and (b) Formality under simultaneous steering.

432 by a start and end index in Qwen2.5-7B-Instruct. When calculating the average score, we applied a
 433 penalty for outputs that collapsed into repetitive, meaningless content. The heatmap reveals a clear
 434 pattern: the most effective control (indicated by the highest positive scores in orange and red) is
 435 concentrated in the mid-to-late layers of the model. Specifically, interventions starting around layer
 436 18 and extending to approximately layer 23 yield the strongest stylistic effect. Intervening in the
 437 initial layers (1-10) proves far less effective and can even be detrimental to the output. This empirical
 438 result aligns with the prevailing hypothesis that later transformer layers encode more abstract
 439 semantic and stylistic information (Zhang et al., 2025). Based on this analysis, we apply steering to
 440 layers 18 through 23 in our main experiments, as this range provides a robust and powerful locus for
 441 style manipulation.

442 4.4 ABLATION STUDIES

443 We conduct an ablation study to validate the necessity of each component
 444 in Causal-Steer. As shown in Table 2, every component is critical for optimal
 445 performance.

446 **Removing the contrastive learning objective (“-w/o Contrast”) causes a**
 447 **notable decline in control effectiveness.** Forgoing the differential activation (“-w/o Difference”) also measurably weakens control. Both results validate our causal intervention strategy. The aggregation pipeline is equally important; removing PCA (“-w/o PCA”) or using a simple arithmetic mean (“-w/o Mean”) degrades performance by failing to properly denoise the style signal. Finally, using only the last token’s representation (“-w/o Mean Token”) instead of averaging across all tokens severely diminishes control intensity, underscoring the need for a holistic style signal. These findings confirm that all components contribute synergistically to the framework’s effectiveness.

448 4.5 MULTI-ATTRIBUTE CONTROL

449 Causal-Steer’s capabilities extend beyond single-attribute manipulation to natural, multi-dimensional style control. This is theoretically grounded in the sparse nature of high-dimensional vector spaces, which permits the linear superposition of multiple style vectors (Liang et al., 2024). By simply adding the vectors for different attributes, we can achieve simultaneous and composable control over the generation process.

450 Figure 7 provides an empirical demonstration of this principle, where we jointly steer for Formality and Conceptual Complexity. The figure presents two heatmaps showing the resulting style scores as a function of the formality coefficient α_1 (horizontal axis) and the knowledge coefficient α_2 (vertical axis). Specifically, Subfigure (a) illustrates the model’s output **Knowledge Difficulty Score**, while Subfigure (b) shows the generated **Formality Score**. The heatmaps demonstrate that as the control signals α_1 and α_2 are varied, the corresponding style scores undergo a **smooth and continuous transition**. Furthermore, the plots reveal a positive correlation between the two attributes. Intensifying one style’s control signal produces a corresponding change in the score for the other style. For example, increasing the conceptual complexity signal (α_2) also tends to increase the formality score, and vice versa. This observation highlights the inherent semantic interplay between advanced conceptual content and formal language. The smooth and predictable gradients across both heatmaps provide strong evidence that Causal-Steer enables fine-grained and continuous control over multiple stylistic dimensions, while effectively capturing their natural associations.

451 4.6 GENERALIZATION TO OTHER CONTROL TASKS

452 To assess the generalizability of Causal-Steer beyond conceptual complexity, we evaluated its performance on two distinct stylistic control tasks: formality control and text detoxification.

453 Table 3 presents the results for Formality task. Causal-Steer demonstrates superior control over the target style, achieving the highest formality score (8.61) when steering towards formal style and

454 **Table 3: Performance of different methods on Formal and Informal datasets.**

Method	Formal					Informal				
	Rel. \uparrow	Flu. \uparrow	Tone. \uparrow	For. \uparrow	PF. \downarrow	Rel. \uparrow	Flu. \uparrow	Tone. \uparrow	For. \downarrow	PF. \downarrow
CAA _{mean}	9.05	6.25	8.12	6.83	0.91	9.28	8.08	5.65	2.30	0.32
RepE _{mean}	9.79	8.47	8.82	6.38	0.96	8.90	6.68	5.59	2.80	0.72
ITI _{mean}	9.73	8.26	8.29	5.86	0.91	7.54	5.12	4.71	2.71	0.78
CLMI	9.80	9.37	9.41	7.58	0.88	8.82	7.70	5.94	2.40	0.36
CS	9.84	8.66	9.55	8.61	0.98	9.38	7.73	5.74	2.22	0.20

486 one of the lowest scores (2.22) when steering towards informal style. Crucially, this high degree of
 487 stylistic control is attained while simultaneously yielding the highest scores for relevance and sci-
 488 entific accuracy, indicating that Causal-Steer effectively modulates style without degrading content
 489 quality.

490 Furthermore, we applied Causal-Steer to the
 491 critical safety task of detoxification with
 492 Llama-2-7b-chat (Touvron et al., 2023b), with
 493 results shown in Table 4. Causal-Steer sig-
 494 nificantly outperforms all baselines, achieving
 495 the lowest toxicity scores on both the toxic
 496 and random test sets, [where both evaluations](#)
 497 [involve one-way detoxification rather than the](#)
 498 [bidirectional control used in our other exper-](#)
 499 [iments.](#) This detoxification performance is
 500 achieved while maintaining a competitive per-
 501 plexity (PPL), suggesting that Causal-Steer ef-
 502 fectively mitigates toxicity without severely compro-
 503 mising the model’s linguistic coherence. These
 504 experiments collectively demonstrate that our pro-
 505 posed vector extraction and steering mechanism
 506 provides a versatile and effective solution for a wide range of attribute control problems. We also
 507 tested Causal-Steer cross-lingually, detailed cases are in Appendix J.

Table 4: Comparison of toxicity control methods on two test sets. Toxicity (lower is better) and perplexity (PPL, lower is better) are reported.

Model	Toxicity _{toxic}		Toxicity _{random}	
	Toxicity ↓	PPL ↓	Toxicity ↓	PPL ↓
Baseline	0.1807	13.71	0.0956	19.23
POSPROMPT	0.1913	59.98	0.1008	18.32
ActAdd	0.1620	34.08	0.0852	12.61
Arithmetic	0.1625	6.84	0.0816	7.34
GCAV-Output	<u>0.0879</u>	21.29	<u>0.0622</u>	6.08
Causal-Steer	0.0609	<u>12.95</u>	0.0520	8.18

Table 5: Comparison of Model Responses

α	Question: Do magnetic and/or electric field have any influence on time and space?
10	Yes,..., Electric and magnetic fields do not directly change spacetime, but they can affect how particles move, which influences how time and distance are measured in practice...
-5	Yes,..., In general relativity, electromagnetic fields contribute to spacetime curvature through their energy, meaning that strong fields can slightly alter the geometry of spacetime...
-20	Yes,..., Within the framework of Einstein’s general relativity, the interaction between electromagnetism and gravity is formally described by the Einstein–Maxwell equations , where the stress–energy tensor of the electromagnetic field directly enters Einstein’s field equations to determine spacetime curvature...

4.7 CASE STUDY

521 Table 5 illustrates representative responses under different control strengths α . As α decreases, the
 522 generated answers gradually shift from intuitive and accessible descriptions to more theoretical and
 523 domain-specific explanations, ranging from practical comments on measurement effects ($\alpha = 10$)
 524 to discussions of spacetime curvature ($\alpha = -5$), and finally to highly academic references such
 525 as the Einstein–Maxwell equations ($\alpha = -20$). This demonstrates that α serves as a continuous
 526 control knob, enabling smooth adjustment of responses along a spectrum from layperson-friendly to
 527 technical. For brevity, we only present a condensed example here, while the complete outputs and
 528 additional cases are provided in the Appendix H.

5 CONCLUSION

533 We introduced **Causal-Steer**, a novel framework for fine-grained style control in LLMs that removes
 534 the dependency on parallel corpora by leveraging LoRA as a causal intervention to disentangle
 535 style vectors. Supported by a robust aggregation pipeline, our method successfully isolates a pure
 536 style signal from non-parallel data. Experimental results demonstrate that Causal-Steer enables
 537 linear, bidirectional, and compositional control over diverse stylistic attributes such as conceptual
 538 complexity and formality, while preserving generation quality and exhibiting strong cross-lingual
 539 adaptability. These findings highlight the practicality and effectiveness of our approach, offering a
 continuous and robust paradigm for adaptive and steerable language models beyond discrete control.

540
541
ETHICS STATEMENT542
543
544
Our research fully adheres to ethical guidelines for responsible AI and machine learning research.
All datasets used in our experiments are publicly available datasets. No proprietary, sensitive, or
private data was used in this study.545
546
547
548
549
In addition to computational experiments, we conducted a small-scale human study to assess text
style. Participation was voluntary, and all participants provided informed consent before taking
part. The study was reviewed and approved under our institution’s internal review procedures, and
participants’ privacy and confidentiality were fully protected. All collected data was anonymized
and used exclusively for research purposes.550
551
552
553
We acknowledge that responsible research entails careful consideration of potential harms and social
impacts. Our work does not involve manipulative, discriminatory, or unsafe practices, and we have
designed our experiments to minimize any negative consequences to participants and the broader
community.555
556
REPRODUCIBILITY STATEMENT557
558
559
560
561
562
563
564
565
566
We have taken several measures to ensure the reproducibility of our work. First, detailed descriptions
of our methods, model architectures, and algorithms are provided in the main text, and the
corresponding code is made available through the anonymous repository <https://anonymous.4open.science/r/cs-01C1>, which is also referenced in the supplementary materials. Sec-
ond, all datasets used in our experiments are publicly available and included in the anonymous
repository, along with complete data processing steps and instructions necessary to replicate our
experiments. Third, in the appendix, we provide detailed explanations of the experimental setup,
hyperparameters, evaluation protocols, including prompt design and review procedures, to allow
accurate replication of our computational and human-in-the-loop experiments. Together, these re-
sources provide all information necessary for reproducing our results.567
568
REFERENCES569
570
571
Takuya Akiba, Makoto Shing, Yujin Tang, Qi Sun, and David Ha. Evolutionary optimization of
model merging recipes. *Nature Machine Intelligence*, 7(2):195–204, 2025.572
573
574
Katherine Atwell, Sabit Hassan, and Malihe Alikhani. Appdia: A discourse-aware transformer-
based style transfer model for offensive social media conversations. *arXiv preprint arXiv:2209.08207*, 2022.575
576
577
Tom Brown, Benjamin Mann, Nick Ryder, Melanie Subbiah, Jared D Kaplan, Prafulla Dhariwal,
Arvind Neelakantan, Pranav Shyam, Girish Sastry, Amanda Askell, et al. Language models are
few-shot learners. *Advances in neural information processing systems*, 33:1877–1901, 2020.578
579
580
Meri Coleman and Ta Lin Liau. A computer readability formula designed for machine scoring.
Journal of Applied Psychology, 60(2):283, 1975.581
582
Jasper Dekoninck, Marc Fischer, Luca Beurer-Kellner, and Martin Vechev. Controlled text genera-
tion via language model arithmetic. *arXiv preprint arXiv:2311.14479*, 2023.583
584
585
Angela Fan, Yacine Jernite, Ethan Perez, David Grangier, Jason Weston, and Michael Auli. Eli5:
Long form question answering. *arXiv preprint arXiv:1907.09190*, 2019.586
587
588
Yujie Feng, Liming Zhan, Zexin Lu, Yongxin Xu, Xu Chu, Yasha Wang, Jiannong Cao, Philip S Yu,
and Xiao-Ming Wu. Geoedit: Geometric knowledge editing for large language models. *arXiv preprint arXiv:2502.19953*, 2025.589
590
591
592
593
Zijian Feng, Hanzhang Zhou, Kezhi Mao, and Zixiao Zhu. FreeCtrl: Constructing control centers
with feedforward layers for learning-free controllable text generation. In Lun-Wei Ku, Andre
Martins, and Vivek Srikumar (eds.), *Proceedings of the 62nd Annual Meeting of the Association
for Computational Linguistics (Volume 1: Long Papers)*, pp. 7627–7640, Bangkok, Thailand,
August 2024. Association for Computational Linguistics. doi: 10.18653/v1/2024.acl-long.412.
URL <https://aclanthology.org/2024.acl-long.412/>.

594 Rudolf Flesch. Flesch-kincaid readability test. *Retrieved October, 26(3):2007, 2007.*
 595

596 Samuel Gehman, Suchin Gururangan, Maarten Sap, Yejin Choi, and Noah A Smith. Real-
 597 toxicityprompts: Evaluating neural toxic degeneration in language models. *arXiv preprint*
 598 *arXiv:2009.11462*, 2020.

599 Google DeepMind Gemini Team. Gemini 2.5: Pushing the frontier with advanced reasoning,
 600 multimodality, long context, and next generation agetic capabilities. *arXiv preprint*, 2025.
 601 *arXiv:2507.06261*.

602

603 Aaron Grattafiori, Abhimanyu Dubey, Abhinav Jauhri, Abhinav Pandey, Abhishek Kadian, Ahmad
 604 Al-Dahle, Aiesha Letman, Akhil Mathur, Alan Schelten, Alex Vaughan, et al. The llama 3 herd
 605 of models. *arXiv preprint arXiv:2407.21783*, 2024.

606

607 Jingxuan Han, Quan Wang, Zikang Guo, Benfeng Xu, Licheng Zhang, and Zhendong Mao. Dis-
 608 entangled learning with synthetic parallel data for text style transfer. In *Proceedings of the 62nd*
 609 *Annual Meeting of the Association for Computational Linguistics (Volume 1: Long Papers)*, pp.
 610 15187–15201, 2024.

611

612 Edward J Hu, Yelong Shen, Phillip Wallis, Zeyuan Allen-Zhu, Yuanzhi Li, Shean Wang, Lu Wang,
 613 Weizhu Chen, et al. Lora: Low-rank adaptation of large language models. *ICLR*, 1(2):3, 2022.

614

615 Gabriel Ilharco, Marco Tulio Ribeiro, Mitchell Wortsman, Suchin Gururangan, Ludwig Schmidt,
 616 Hannaneh Hajishirzi, and Ali Farhadi. Editing models with task arithmetic. *arXiv preprint*
 617 *arXiv:2212.04089*, 2022.

618

619 Sara Kangaslahti and David Alvarez-Melis. Continuous language model interpolation yields dy-
 620 namic and controllable text generation. *Transactions on Machine Learning Research*, 2025.

621

622 Tassilo Klein and Moin Nabi. Contrastive perplexity for controlled generation: An application in
 623 detoxifying large language models. *arXiv preprint arXiv:2401.08491*, 2024.

624

625 Kenneth Li, Oam Patel, Fernanda Viégas, Hanspeter Pfister, and Martin Wattenberg. Inference-
 626 time intervention: Eliciting truthful answers from a language model. In A. Oh, T. Nau-
 627 mann, A. Globerson, K. Saenko, M. Hardt, and S. Levine (eds.), *Advances in Neural*
 628 *Information Processing Systems*, volume 36, pp. 41451–41530. Curran Associates, Inc.,
 629 2023. URL https://proceedings.neurips.cc/paper_files/paper/2023/file/81b8390039b7302c909cb769f8b6cd93-Paper-Conference.pdf.

630

631 Xun Liang, Hanyu Wang, Yezhaohui Wang, Shichao Song, Jiawei Yang, Simin Niu, Jie Hu, Dan
 632 Liu, Shunyu Yao, Feiyu Xiong, et al. Controllable text generation for large language models: A
 633 survey. *arXiv preprint arXiv:2408.12599*, 2024.

634

635 Pengfei Liu, Weizhe Yuan, Jinlan Fu, Zhengbao Jiang, Hiroaki Hayashi, and Graham Neubig. Pre-
 636 train, prompt, and predict: A systematic survey of prompting methods in natural language pro-
 637 cessing. *ACM computing surveys*, 55(9):1–35, 2023.

638

639 Oscar Mañas, Pierluca D’Oro, Koustuv Sinha, Adriana Romero-Soriano, Michal Drozdzal, and
 640 Aishwarya Agrawal. Controlling multimodal llms via reward-guided decoding. *arXiv preprint*
 641 *arXiv:2508.11616*, 2025.

642

643 G Harry Mc Laughlin. Smog grading-a new readability formula. *Journal of reading*, 12(8):639–646,
 644 1969.

645

646 OpenAI. Introducing gpt-4.1 in the api. OpenAI blog, 2025. URL <https://openai.com/index/gpt-4-1/>. Accessed: 2025-09-24.

647

648 Long Ouyang, Jeff Wu, Xu Jiang, Diogo Almeida, Carroll Wainwright, Pamela Mishkin, Chong
 649 Zhang, Sandhini Agarwal, Katarina Slama, Alex Ray, et al. Training language models to follow
 650 instructions with human feedback. *Advances in Neural Information Processing Systems*, 35:
 651 27730–27744, 2022.

648 Qwen, An Yang, Baosong Yang, Beichen Zhang, Binyuan Hui, Bo Zheng, Bowen Yu, Chengyuan
 649 Li, Dayiheng Liu, Fei Huang, Haoran Wei, Huan Lin, Jian Yang, Jianhong Tu, Jianwei Zhang,
 650 Jianxin Yang, Jiaxi Yang, Jingren Zhou, Junyang Lin, Kai Dang, Keming Lu, Keqin Bao, Kexin
 651 Yang, Le Yu, Mei Li, Mingfeng Xue, Pei Zhang, Qin Zhu, Rui Men, Runji Lin, Tianhao Li,
 652 Tianyi Tang, Tingyu Xia, Xingzhang Ren, Xuancheng Ren, Yang Fan, Yang Su, Yichang Zhang,
 653 Yu Wan, Yuqiong Liu, Zeyu Cui, Zhenru Zhang, and Zihan Qiu. Qwen2.5 technical report, 2024.
 654 Preprint.

655 Nina Rimsky, Nick Gabrieli, Julian Schulz, Meg Tong, Evan Hubinger, and Alexander Turner.
 656 Steering llama 2 via contrastive activation addition. In Lun-Wei Ku, Andre Martins, and
 657 Vivek Srikumar (eds.), *Proceedings of the 62nd Annual Meeting of the Association for Com-
 658 putational Linguistics (Volume 1: Long Papers)*, pp. 15504–15522, Bangkok, Thailand, August
 659 2024. Association for Computational Linguistics. doi: 10.18653/v1/2024.acl-long.828. URL
 660 <https://aclanthology.org/2024.acl-long.828/>.

661 Hugo Touvron, Louis Martin, Kevin Stone, Peter Albert, Amjad Almahairi, Yasmine Babaei, Niko-
 662 lay Bashlykov, Soumya Batra, Prajjwal Bhargava, Shruti Bhosale, et al. Llama 2: Open founda-
 663 tion and fine-tuned chat models. *arXiv preprint arXiv:2307.09288*, 2023a.

664 Hugo Touvron, Louis Martin, Kevin R. Stone, Peter Albert, Amjad Almahairi, Yasmine Babaei,
 665 Nikolay Bashlykov, Soumya Batra, Prajjwal Bhargava, Shruti Bhosale, Dan Bikel, Lukas Blecher,
 666 Cristian Canton Ferrer, Moya Chen, Guillem Cucurull, David Esiobu, Jude Fernandes, Jeremy Fu,
 667 Wenyin Fu, Brian Fuller, Cynthia Gao, Vedanuj Goswami, Naman Goyal, Anthony Hartshorn,
 668 Saghar Hosseini, Rui Hou, Hakan Inan, Marcin Kardas, Viktor Kerkez, Madian Khabsa, Isabel
 669 Kloumann, Artem Korenev, Punit Singh Koura, Marie-Anne Lachaux, Thibaut Lavril, Jenya Lee,
 670 Diana Liskovich, Yinghai Lu, Yuning Mao, Xavier Martinet, Todor Mihaylov, Pushkar Mishra,
 671 Igor Molybog, Yixin Nie, Andrew Poulton, Jeremy Reizenstein, Rashi Rungta, Kalyan Saladi,
 672 Alan Schelten, Ruan Silva, Eric Michael Smith, Ranjan Subramanian, Xia Tan, Binh Tang, Ross
 673 Taylor, Adina Williams, Jian Xiang Kuan, Puxin Xu, Zheng Yan, Iliyan Zarov, Yuchen Zhang,
 674 Angela Fan, Melanie Kambadur, Sharan Narang, Aurelien Rodriguez, Robert Stojnic, Sergey
 675 Edunov, and Thomas Scialom. Llama 2: Open foundation and fine-tuned chat models. *arXiv*
 676 preprint, 2023b. *arXiv:2307.09288*.

677 Alexander Turner, Ian Gemp, Andreea-Maria Rusu, James Moulder, George Toderici, Ivan Timo-
 678 feev, Brandon O’Donoghue, and Cagan Anil. Steering language models with activation engineer-
 679 ing. *arXiv preprint arXiv:2312.01633*, 2023a.

680 Alexander Matt Turner, Lisa Thiergart, Gavin Leech, David Udell, Juan J Vazquez, Ulisse Mini, and
 681 Monte MacDiarmid. Activation addition: Steering language models without optimization. *arXiv
 682 e-prints*, pp. arXiv–2308, 2023b.

683 Lev S Vygotsky. *Mind in society: The development of higher psychological processes*. Harvard
 684 university press, 1978.

685 Qingsong Wang, Tao Wu, Wang Lin, Yueying Feng, Gongsheng Yuan, Chang Yao, and Jingyuan
 686 Chen. Cognitive-level adaptive generation via capability-aware retrieval and style adaptation.
 687 *arXiv preprint arXiv:2509.19336*, 2025. Accepted to Findings of EMNLP 2026.

688 Zhengxuan Wu, Aryaman Arora, Zheng Wang, Atticus Geiger, Dan Jurafsky, Christopher D Man-
 689 ning, and Christopher Potts. Reft: Representation finetuning for language models. 2024. URL
 690 <https://arxiv.org/abs/2404.03592>.

691 Hanyu Zhang, Xiting Wang, Chengao Li, Xiang Ao, and Qing He. Controlling large language
 692 models through concept activation vectors. In *Proceedings of the AAAI Conference on Artificial
 693 Intelligence*, volume 39, pp. 25851–25859, 2025.

694 Yi Zhang, Tao Ge, and Xu Sun. Parallel data augmentation for formality style transfer. *arXiv
 695 preprint arXiv:2005.07522*, 2020.

696 Andy Zou, Long Phan, Sarah Chen, James Campbell, Phillip Guo, Richard Ren, Alexander Pan,
 697 Xuwang Yin, Mantas Mazeika, Ann-Kathrin Dombrowski, et al. Representation engineering: A
 698 top-down approach to ai transparency. *arXiv preprint arXiv:2310.01405*, 2023.

702 A STATEMENT ON THE USE OF LLMs
703704 We report the use of a large language model in the preparation of this manuscript. Specifically, we
705 used Gemini 2.5 (Gemini Team, 2025) to identify and correct grammatical errors and to improve the
706 overall readability of the text. The authors retained full responsibility for all content, and the final
707 version of the paper reflects our own edits and revisions.
708709 B DETAILS OF EXPERIMENTAL CONFIGURATION
710711 To ensure the reproducibility of our results, we provide a detailed description of the experimental
712 configuration used for training, inference, and evaluation. All experiments were conducted on four
713 NVIDIA A100 GPUs with 80GB memory each. Our model was trained for a total of 2 epochs
714 with a per-device batch size of 8, a learning rate of 1×10^{-4} , gradient accumulation steps set to 1,
715 and a maximum sequence length of 512 tokens. For parameter-efficient fine-tuning, we employed
716 Low-Rank Adaptation (LoRA) with a rank $r = 8$, scaling factor $\alpha = 16$, and a dropout rate of 0.05.
717 The PEFT library was used to automatically identify and adapt the appropriate linear layers within
718 the model. In addition, a contrastive learning objective was incorporated with the contrastive loss
719 weight $\lambda = 0.05$. For inference, we used deterministic decoding (greedy search without sampling)
720 with a maximum generation length of 512 tokens. During evaluation with GPT-based scoring, the
721 temperature was set to 0.2 to ensure stability and consistency of judgments.
722723 C DETAILS OF BASELINES
724725 We benchmark our method against a comprehensive suite of baselines for controllable generation,
726 categorized into prompt-based and activation-based approaches. For our primary task of conceptual
727 complexity control, we include zero-shot instructional prompting and three prominent activation
728 steering methods: Representation Engineering (RepE) (Zou et al., 2023), Contrastive Activation Ad-
729 dition (CAA) (Turner et al., 2023a), and Inference-Time Intervention (ITI) (Li et al., 2023). Distinct
730 from these activation-based techniques, we also include Continuous Language Model Interpol-
731 ation(CLMI) (Kangaslahti & Alvarez-Melis, 2025) for our main experiment, which achieves control
732 by interpolating the weights of Low-Rank Adapters (LoRA) rather than steering activations. For
733 the activation-based methods, we evaluate both the standard approach using the final token’s hid-
734 den state and a stronger variant we implement that averages hidden states across all tokens (**-avg**).
735 For the toxicity detoxification task, we include additional specialized baselines such as the prompt-
736 based POSPROMPT and activation steering methods including Arithmetic (Dekoninck et al., 2023),
737 ActAdd (Turner et al., 2023b), and GCAV-Output (Zhang et al., 2025).
738739 D DETAILS OF DATASETS
740741 We evaluate our method on a primary task of controlling conceptual complexity and assess its gen-
742 eralizability on two additional stylistic dimensions: toxicity detoxification and formality control.
743744 For our primary task, conceptual complexity, we extract the corresponding style vector from the
745 **Scale**³, a question-answering corpus with graded difficulty levels. We then evaluate the model’s
746 ability to modulate content difficulty on a test set of 100 questions randomly sampled from the
747 **ELI5** dataset (Fan et al., 2019).
748749 To demonstrate the versatility of our method, we conduct two generalization experiments. For tox-
750 icality control, we derive the style vector from the **APPDIA** dataset (Atwell et al., 2022), which pro-
751 vides aligned toxic and detoxified sentence pairs. We evaluate its performance following the setup
752 of Zhang et al. (2025) on two subsets of the **RealToxicityPrompts** corpus (Gehman et al., 2020):
753 one with highly toxic prompts and another with randomly sampled ones. For formality control, we
754 extract the style vector from 16,000 sentence pairs randomly sampled from the parallel corpus of
Zhang et al. (2020).
755³<https://huggingface.co/wa57/Scale>

756 Since both the APPDIA and formality datasets are originally composed of parallel sentences rather
 757 than question–answer pairs, we adapt them to the instruction-following setting: we use **GPT-4.1** to
 758 generate corresponding questions q for each pair and slightly modify the answers to better align with
 759 instruct-style training. The exact prompting procedure is detailed in Appendix G.1, and the adapted
 760 datasets are provided both in the appendix and via our anonymous repository.

766 E HUMAN EVALUATION

770 To better assess the relative performance of our
 771 method, we conducted a human evaluation us-
 772 ing a Best-Worst Scaling methodology. This
 773 approach reduces annotator bias compared to
 774 direct scoring. For each of the 50 test ques-
 775 tions, 3 annotators were shown the *Simple* and
 776 *Complex* outputs from our method, CAA_{mean} ,
 777 and CLMI in a randomized, blind setting. For
 778 each set of three, they were asked to select the
 779 single “Best” and “Worst” response based on a
 780 holistic judgment of style appropriateness and
 781 overall quality (e.g., fluency, coherence).

782 The results, summarized in Table 6, show a
 783 strong preference for our method. For the *Com-
 784 plex* style, our model was chosen as “Best” in a decisive **65.3%** of cases, significantly outperforming
 785 CAA_{mean} (23.3%) and CLMI (11.3%).

786 A similar trend was observed for the *Simple* style, where our method was again preferred as “Best”
 787 in **59.3%** of evaluations. This confirms its robust bidirectional control. The low percentage of our
 788 method being selected as “Worst” (1.3% for Complex and 14.0% for Simple) further underscores
 789 its stability and reliability. In contrast, CLMI was rated “Worst” in the majority of cases (63.3% for
 790 Complex), highlighting its limitations in achieving effective style control. These findings from our
 791 comparative human evaluation strongly validate the superiority of our proposed framework.

796 F COMPUTATIONAL OVERHEAD

800 The primary computational cost of our framework is in-
 801 incurred during the offline style vector extraction phase. In
 802 contrast, the overhead during online inference is negligi-
 803 ble. As shown in Table 7, the generation speed, measured
 804 in tokens per millisecond, remains nearly identical to the
 805 baseline even when applying multiple steering vectors si-
 806 multaneously. The control intensity (α) has no impact on
 807 this speed, as the underlying operation is a simple vector
 808 addition. This efficient design, which concentrates com-
 809 putational effort into a one-time offline process, makes
 our method highly practical for real-time applications.

Table 6: Human evaluation results based on Best-Worst ranking. We report the percentage of times each method was chosen as Best, Middle, or Worst by 3 annotators across 50 questions. A higher ‘Best’ percentage indicates stronger preference.

Method	Complex Style (%)			Simple Style (%)		
	Best	Middle	Worst	Best	Middle	Worst
CLMI	11.3	25.3	63.3	14.7	28.0	57.3
CAA_{mean}	23.3	41.3	35.3	26.0	45.3	28.7
Ours	65.3	33.3	1.3	59.3	26.7	14.0

Table 7: Inference speed in tokens per millisecond (tokens/ms). Higher values are better. Our method maintains a speed comparable to the baseline.

Configuration	Speed (tokens/ms)
Baseline	1.17
1 vector, $\alpha = 20$	1.13
1 vector, $\alpha = 30$	1.16
2 vectors, $\alpha = 20$	1.12
2 vectors, $\alpha = 30$	1.04

810 **G PROMPTS**
811812 **G.1 PROMPTS FOR DATASETS REWRITE**
813814
815 Transform the given pair of parallel sentences (e.g., formalinformal, toxicdetoxified) into a unified QA
816 format.

817 Steps

818 1. Generate one natural and coherent question (Q) that could reasonably elicit both given answers.
819 2. Produce two answers (A1 and A2) corresponding to the styles in the original parallel data:
820 – If the pair is formal vs. informal, ensure that A1 is informal and A2 is formal.
821 – If the pair is toxic vs. detoxified, ensure that A1 retains the toxic style while A2 provides the detoxified
822 version.
823 3. You may expand the answers with additional content to increase richness, but keep both answers
824 semantically consistent with each other.
825 4. Always preserve the intended style (informal vs. formal; toxic vs. detoxified).826 **G.2 PROMPTS FOR CONCEPTUAL COMPLEXITY TASK**
827828 You are an expert evaluator for natural language generation quality.
829

830 Evaluate the following text based on four dimensions. Focus especially on conceptual complexity.

831 1. Relevance: Does the response stay on topic and directly address the question or topic without irrelevant
832 content?
833 2. Fluency: Is the language clear, coherent, and easy to read, with proper grammar and logical flow?
834 3. Scientific Accuracy: Are the knowledge points and explanations factually correct and reliable based on
835 authoritative sources?
836 4. Knowledge Difficulty: Assess whether the knowledge level matches the expected difficulty.
837 – Higher scores: Highly technical or research-level content suitable for graduate-level understanding.
838 – Lower scores: Simple, introductory, or popular-science level explanations.
839 Give each dimension a score from 1 (poor) to 10 (excellent).840 **G.3 PROMPTS FOR FORMALITY TASK**
841842 You are an expert evaluator for natural language generation quality.
843

844 Evaluate the following text based on four dimensions. Focus especially on formality.

845 1. Relevance: Does the response stay on topic and directly address the question or topic without irrelevant
846 content?
847 2. Fluency: Is the language clear, coherent, and easy to read, with proper grammar and logical flow?
848 3. Tone Appropriateness: Is the tone of the response (e.g., professional, casual, empathetic, neutral)
849 suitable for the prompt’s context and implied audience?
850 4. Formality: Assess the text’s level of formality based on word choice, sentence structure, and adherence
851 to stylistic conventions.(Assign a score of 5 for standard model output.)
852 – Higher scores: Highly formal language, sophisticated vocabulary, complex sentence structures, and an
853 objective tone. Avoids slang, contractions, and colloquialisms.
854 – Lower scores: Highly informal or conversational language. May use slang, contractions, simple
855 sentence structures, and a personal or subjective tone.
856 Give each dimension a score from 1 (poor) to 10 (excellent).

864 H CASE OF CONCEPTUAL COMPLEXITY TASK

865
866 **Question:** Do magnetic and/or electric fields have any influence on time and space?
867

868 $\alpha = 10$ (Simple)
869

870 Yes, both the electric and magnetic fields can affect how we measure time and distance in certain situations
871 , especially when dealing with very fast speeds close to light or strong gravitational fields.
872

873 1.**Electric Field**: In general relativity, an electric charge at rest creates no direct effect on spacetime
874 that would change our usual way of measuring distances and times (like using clocks). However, if
875 you consider charged particles moving through an electromagnetic field, it's important to remember
876 that they experience forces from those fields which could make their paths twist around as seen from
877 other frames of reference. But this doesn't directly mean there is a change in the measurement of
878 time and space for them; rather, it means that things get more complicated because now you need to
879 take into account not just gravity but also these extra forces coming from the electric charges.
880

881 2.**Magnetic Field**: Similar to the case with electric fields, a single magnet sitting still won't cause
882 changes in measurements of time and space unless something else interacts with its field. When
883 considering objects moving near each other under the influence of magnets, like two wires carrying
884 current, then yes, the movement of one wire affects another due to the changing magnetic field,
885 making everything move differently than expected without taking the magnetic force into
886 consideration. This makes the path taken look different depending where you're standing kind of like
887 seeing someone walk diagonally instead of straight ahead while riding on a merry-go-round!
888

889 3.**Spacetime Curvature Due To EM Energy**: Just like mass curves spacetime according to General
890 Relativity, energy carried by photons (light) does so too. So having lots of electricity and magnetism
891 swirling about will curve spacetime slightly, much like putting a heavy ball down onto a trampoline
892 causes it to bend downwards. It might be tiny bending compared to planets and stars, but it exists!
893

894 In summary, while individual static electric and magnetic fields don't usually warp time and space
895 themselves, once you start talking about moving charges.
896

897 $\alpha = -5$ (Medium)
898

899 Yes, both the electromagnetic fields (electric and magnetic) can indeed affect spacetime according to
900 modern physics theories, particularly general relativity.
901

902 In Albert Einstein's theory of General Relativity, gravity is described as curvature in spacetime caused by
903 mass and energy. This means that not only does massive matter curve spacetime but also strong or
904 dynamic electromagnetic fields can contribute to this curvature under certain conditions. Specifically:
905

906 1. **Einstein–Maxwell Equations**: These equations combine Maxwell's equations for electromagnetism
907 with Einstein's field equations from general relativity. They describe how an electromagnetic field
908 affects the geometry of spacetime through its stress–energy tensor term.
909

910 2. **Gravitomagnetic Effects**: In extreme scenarios involving very high currents or intense magnetic
911 fields, there could be significant gravitomagnetic effects predicted by these unified models. However,
912 such effects would typically require extremely large-scale phenomena beyond what we encounter in
913 everyday situations.
914

915 3. **Quantum Gravity Theories**: At quantum scales, where gravitational forces become comparable to
916 other fundamental interactions like those mediated by the electromagnetic force, more speculative
917 theoretical frameworks may come into play. Some proposals within loop quantum gravity or string
918 theory suggest that even at microscopic levels, electromagnetic fields might influence spacetime
919 structure indirectly via their contributions to the overall quantum state of spacetime.
920

921 4. **Experimental Observations**: While direct experimental evidence supporting these predictions
922 remains limited due to technological constraints, indirect observations and precision measurements
923 continue to refine our understanding of how strongly coupled systems behave near black holes or
924 neutron stars in environments characterized by highly relativistic and possibly magnetized conditions.
925 It's important to note that while theoretically possible, the practical implications of electromagnetic
926 influences on spacetime remain largely confined to astrophysical contexts rather than macroscopic
927 terrestrial environments. Nonetheless, ongoing research continues to explore these fascinating
928 intersections between electrodynamics and gravitational physics.
929

918 $\alpha = -20$ (Complex)
919920 Yes, both electromagnetic fields (which encompass the electric and magnetic fields) can indeed exert
921 influences on spacetime within certain theoretical frameworks of modern physics.
922923 **### Electromagnetic Fields in General Relativity**924 In the context of general relativity, formulated by Albert Einstein, gravitational effects are described
925 through the curvature of spacetime. However, this framework primarily accounts for mass–energy
926 contributions to such curvature. Recent interpretations and extensions of these theories incorporate
927 electrodynamics into considerations of spacetime structure:928 1. ****Quantum Gravity Theories**:** These speculative frameworks attempt to reconcile quantum mechanics
929 with general relativity. In some models, quantized electromagnetic interactions could contribute non
930 trivially to spacetime metrics at microscopic scales.
931 2. ****Non-Linear Electrodynamics**:** Certain modifications or nonlinear formulations of classical
932 electromagnetism predict deviations from Maxwellian predictions under extreme conditions relevant
933 to high-field regimes near black holes or compact astrophysical objects.934 **### Quantum Electrodynamical Effects**935 At the microscale, phenomena governed by quantum electrodynamics (QED), which is an extension of
936 classical electrodynamics incorporating principles of quantum mechanics, exhibit significant
937 implications:938 1. ****Casimir Effect**:** This phenomenon arises due to quantum fluctuations in vacuum states between two
939 closely spaced conductive surfaces. It involves spatial configurations influenced by electromagnetic
940 boundary conditions, manifesting as measurable physical forces.
941 2. ****Vacuum Polarization**:** Within QED, virtual particle pairs (electrons and positrons) transiently
942 interact with intense electromagnetic fields, leading to observable macroscopic consequences via
943 renormalization parameters.944 **### Lorentz Violations and Anisotropic Spacetimes**945 Theoretical explorations often invoke violations of local Lorentz symmetry spatial isotropy and temporal
946 homogeneity postulated foundational tenets of special relativistic formalisms to model emergent
947 phenomenological descriptions consistent with experimental data across various energy scales.948

I CASE OF FORMALITY TASK

949 **Question:** why do most bipedal robots always keep their knees bent a bit when standing?950 $\alpha = -25$ (Informal)951 Most bipedal robots keep their knees slightly bent for several reasons:
952953 1. ****Stability**:** Keeping the legs in a slight bend helps with balance and stability. When the robot is
954 standing still or walking, this position makes it easier to stay upright without falling over.
955 2. ****Energy Efficiency**:** A little bend in the knee can help save energy because it's not as hard on the
956 motors that move the leg parts (like servos). It's like how you might bend your knees before jumping
957 it uses less power but gives more push-off force.
958 3. ****Shock Absorption**:** Just like humans, bending at the knees can act as a shock absorber during steps
959 or jumps. This means the robot doesn't have to work so hard to handle bumps or uneven ground.
960 4. ****Flexibility \& Range of Motion**:** Bending the knees keeps them from getting stuck straight up or
961 down all the time. This lets the robot be more flexible about where its feet go next, which is important
962 if it needs to walk around stuff or change directions fast.
963 5. ****Less Stress On Joints And Bones**:** In real life, keeping joints loose instead of locked up stops
964 things from breaking under pressure. Same goes for these bots – they don't want metal bones
965 snapping!966 So basically, just like we use our bodies' bends to feel comfy and strong while standing, robots get way
967 into those same tricks too!968
969
970
971

972 $\alpha = -10$

973

974

975

976

977

Most bipedal robots maintain a slight bend in their knees while standing for several reasons:

1. **Stability**: Keeping the legs at an angle (bent) helps distribute weight more evenly and provides better stability against tipping over. This is similar to how humans stand with slightly bent knees.
2. **Energy Efficiency**: A small amount of knee flexion can help store potential energy as elastic strain in the leg muscles or tendons. When walking or running, this stored energy can be released to assist in propelling the robot forward, making it more efficient.
3. **Shock Absorption**: The slight bend acts like a shock absorber during movement. It reduces impact forces on both joints and other parts of the body, which could otherwise cause damage from repeated hard landings.
4. **Joint Health**: Maintaining some degree of joint flexibility prevents stiffness that might occur if they were locked straight all the time. Stiffness increases wear and tear on mechanical components.
5. **Control Precision**: In robotics, keeping certain angles allows engineers to fine-tune control algorithms because there's less chance of hitting physical limits compared to having fully extended limbs where you'd hit "hard stops."
6. **Humanoid Design Consistency**: For humanoid robots designed to mimic human movements, maintaining a natural stance makes them look more lifelike and easier to interact with since people expect others to have naturally curved postures rather than rigidly upright ones.

Overall, these factors contribute to improving performance, longevity, and user interaction for bipedal robots!

995 $\alpha = 10$

996

997

998

999

Most bipedal robots maintain a slight bend in the knee for several reasons related to stability and efficiency :

1. **Stability**: A slightly bent posture helps improve balance and stability. This is similar to how humans naturally stand with some degree of flexion at the knees. The bending allows the robot's center of mass to be more centrally positioned over its base, reducing the risk of tipping or falling.
2. **Energy Efficiency**: Bent knees can help reduce energy consumption during static stance phases. By maintaining this position, the mechanical systems (such as motors) require less effort to support the weight of the body without additional strain on joints that might occur if they were fully extended.
3. **Dynamic Stability During Movement**: When performing dynamic movements such as walking or running, having flexible joint angles like those found in human anatomy enables better control and adaptability. Bipedal robots often use these principles to enhance their ability to navigate various terrains and respond to external forces dynamically.
4. **Biological Inspiration**: Many robotic designs draw inspiration from biological models, including human locomotion patterns. Mimicking natural postures can lead to more effective and efficient movement strategies.
5. **Reduction of Stress on Joints and Components**: Keeping certain joints moderately flexed reduces stress on both the physical components within the robot and potential wear and tear associated with prolonged periods of full extension.

These factors collectively contribute to why many bipedal robots adopt a posture involving mild knee bends while standing or moving. However, specific design choices may vary based on the intended application, capabilities, and goals of each individual robot model.

1019

1020

1021

1022

1023

1024

1025

1026 $\alpha = 20$ (Formal)
10271028 Most bipedal robots maintain a slight bend in the knee for several reasons:
1029

1. **Stability and Balance**: Bending the knees slightly helps to enhance stability and balance. This posture allows the robot to distribute its weight more effectively across the lower limbs, reducing the risk of tipping or imbalance.
2. **Postural Adaptation**: Human beings naturally adopt such postures due to biomechanical advantages that facilitate efficient movement and support various activities. Similarly, robotic designs often mimic human postures to improve functionality and adaptability.
3. **Flexibility and Dexterity**: A slight bend in the knees provides greater flexibility and dexterity, enabling the robot to perform a wider range of actions with ease. It facilitates movements such as walking, climbing, and manipulation tasks.
4. **Energy Efficiency**: Bent knees can contribute to energy efficiency during locomotion by allowing smoother transitions between different phases of gait (such as stance phase and swing phase).
5. **Safety Considerations**: Maintaining an upright yet flexible posture reduces stress on joints and musculature over prolonged periods, which is crucial for long-term operation without fatigue or damage.
6. **Mimicry of Natural Movements**: Many robotic systems aim to emulate natural human behaviors to better integrate them into environments where they interact closely with humans, thereby enhancing social acceptability and effectiveness.

1047 These factors collectively explain why many bipedal robots employ a posture characterized by mild flexion
1048 at the knees while maintaining other aspects similar to those observed in human physiology.

1049
1050
1051
1052
1053
1054
1055
1056
1057
1058
1059
1060
1061
1062
1063
1064
1065
1066
1067
1068
1069
1070
1071
1072
1073
1074
1075
1076
1077
1078
1079

1080 **J CASE OF CROSS-LANGUAGE GENERALIZATION**

1081
 1082 To further evaluate the cross-lingual capability of our model, we tested whether activation vectors
 1083 extracted from English datasets could control formality in **German** question-answering tasks. The
 1084 experimental results, presented below, demonstrate that our activation vectors effectively generalize
 1085 across languages, maintaining robust control over stylistic attributes in the target language.
 1086

1087 **Question:** Die globale Finanzkrise von 2007/2008. Wird es eine weitere geben?

1088 $\alpha = 20$ (Informal)

1089
 1090 Es ist schwierig zu sagen, wann und wie das nchste groe Finanzspielzeug wird, aber man kann sicher sein,
 1091 dass es immer noch Risiken gibt, die dazu fhren knnen, dass der Markt pltzlich in Schwierigkeiten
 1092 gert.
 1093

1094 Hier sind einige Grnde, warum ein neuer Finanzschlafmtze vielleicht kommen knnte:

1095 1. **Hilfsschlafmtzen:** Wenn jemand versucht, den Markt mit Hilfe von Geld aus dem Nichts machen
 1096 will – sozusagen einen groen Spielball fr sich selbst – dann kann das zum nchsten groen
 1097 Schlafmtzenspiel werden.

1098 *Beispiel:* Wie bei den Hauseinlagen, die vor vielen Jahren als super–sicher gedacht wurden, aber im
 1099 Endeffekt viele Leute tiefen Schlfer aufwachen lieen, wenn sie ihre Hausgeldkarten nicht gut genug
 1100 versteckt hielten oder vergaen, dass sie gar kein echtes Geld waren!

1101 2. **Zu viel Geld suchen nach einem Ort, um zu spielen:**

1102 *Wenn alle Banken und andere Menschen, die Geld haben wollen, keine gute Idee finden, wo sie ihr Geld
 1103 lassen sollen, dann knnten sie versuchen, etwas ganz Neues zu finden!*

1104 3. **Menschen, die glauben, dass alles okay ist:**, wenn es nicht wirklich okay ist:

1105 *Wie wenn du weit, dass dein Auto kaputt ist, aber du fhrst trotzdem damit, weil du denkt, dass es schon
 1106 lange keinen Fehler gemacht hat.*

1107 4. **Ganze Lnder, die dummspielen:**

1108 *Was passiert, wenn alle Leute in einer Stadt oder Land, das sehr viel Geld hat, einfach nur Spa haben
 1109 wollen, ohne richtig darber nachdenken, was genau sie tun? Es wre wie wenn alle Freunde in deinem
 1110 Kindergarten zusammenhelfen wrden, um ein riesiges Sandburg–Haus zu bauen, aber niemandem
 1111 kommt in den Kopf, dass es Zeit ist, mal rber zur Wasserbrunnen–Schaukel zu gehen!*

1112 $\alpha = -20$ (Formal)

1113
 1114 Es ist schwierig zu sagen, ob und wann genau eine neue Finanzkrise passieren wird, aber wir knnen
 1115 sicherstellen, dass das Risiko immer da ist. Hier sind einige Punkte zum Thema Finanzrisiken:

1116 1. **Lernende Systeme:** Nach der groen Krise von 2007/2008 haben viele Lnder und Banken versucht,
 1117 ihre Systeme besser zu machen. Das bedeutet nicht, dass sie perfekt sind oder nie wieder Probleme
 1118 haben werden.

1119 2. **Debt–Bubble:** Eine groe Schuldenbombe kann sich bauen, wie in den Jahren vor dem Crash. Wenn
 1120 Leute, Unternehmen oder Regierungen zu viel Geld leihen, ohne genug Kredite zurckzahlen zu
 1121 knnen, kann das zu einem Problem fhren.

1122 3. **Housing–Markt–Schwankungen:** Immobilienblscherei war ein groer Teil des Problems im Jahr
 1123 2007/2008. Wenn der Immobilienmarkt pltzlich abfllt, kann das einen Sturz starten.

1124 4. **Technologiefirmen:** Heutzutage gibt es andere Sektoren, die riesige Betten voller Geld haben
 1125 knnen z.B. Tech–Firmen mit hohen Bewertungen. Ein Schlag fr diese Firmen knnte alles verndern.

1126 5. **Klimawandel:** Die Vernderte Weltwirtschaft durch den Klimawandel kann auch zu neuen Art von
 1127 Krisen fhren, die uns berraschen knnten.

1128 6. **Politik und Rechtswesen:** Politische Unruhe und Schwierigkeiten bei der Steuerung von
 1129 Marktsystemen knnen auch dazu fhren, dass Dinge aus dem Ruder laufen.

1130 Um solche Krisen zu verhindern oder wenigstens zu dmpfen, mssen Lnder und Institutionen stndig
 1131 aufpassen und sich anpassen. Es hilft auch, wenn jeder seine eigene finanzielle Situation gut
 1132 kontrolliert und keine zu vielen Risiken nimmt. Insgesamt ist es wichtig, dass alle Beteiligten
 1133 vorsichtig bleiben und immer nach besseren Mglichkeiten suchen, um Risiken zu minimieren.

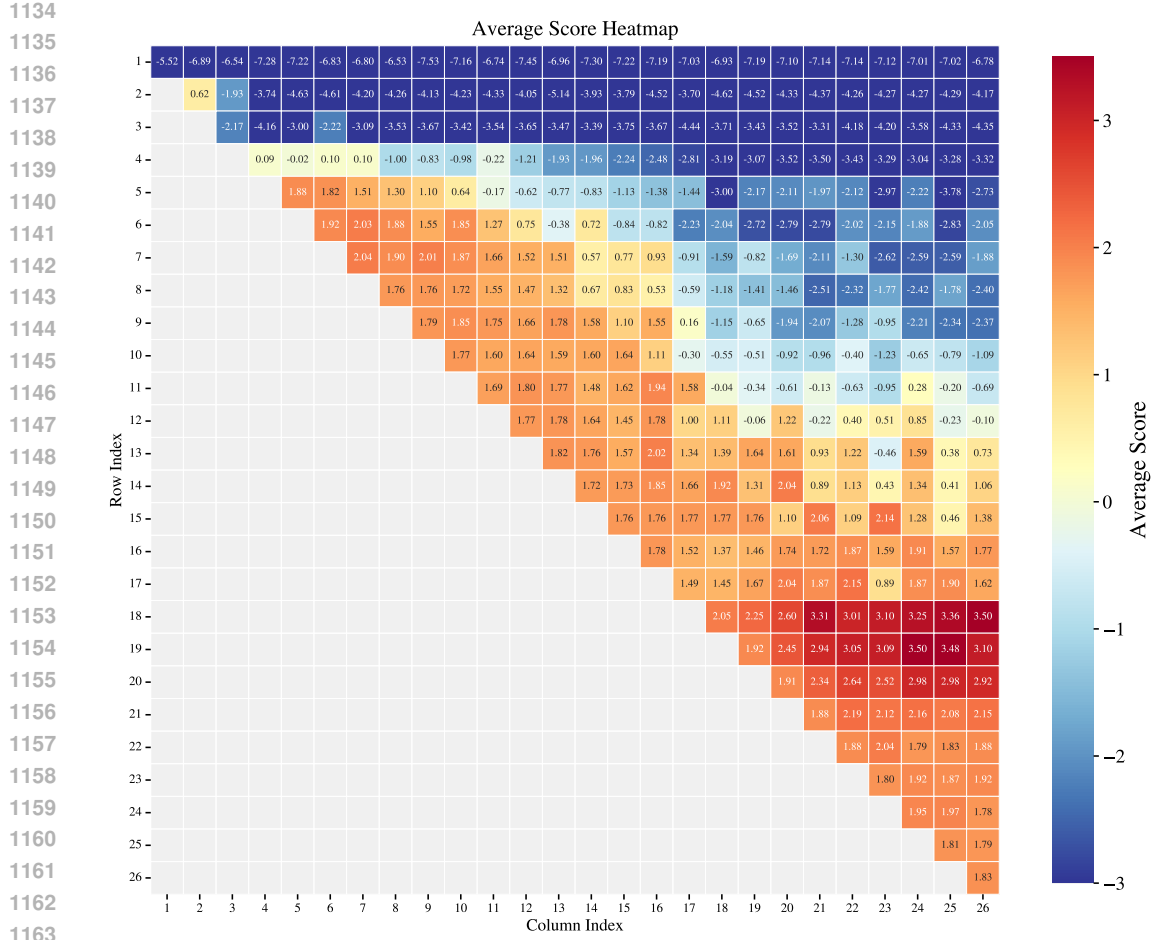


Figure 6: **Heatmap of average style control scores across layer blocks.** The y-axis and x-axis represent the start and end indices for the intervention block, respectively. Scores are averaged over multiple runs.

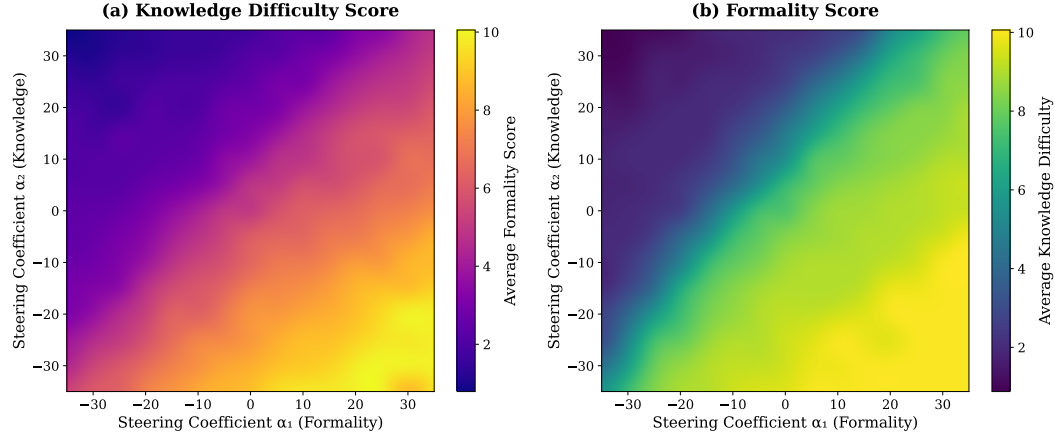


Figure 7: **Two-Dimensional Stylistic Control.** Model output scores for (a) Knowledge Difficulty and (b) Formality under simultaneous steering.